Published in final edited form as:
J Am Chem Soc. 2009 November 25; 131(46): 16771–16778. doi:10.1021/ja904976r.

Laser Photolysis of Dye-Sensitized Nanocapsules Occurs via a Photothermal Pathway

Kimberly A. Dendramis and **Daniel T. Chiu***
Department of Chemistry, University of Washington, Seattle, WA 98195

Abstract

Light-addressable nanocapsules offer a powerful method for delivering spatiotemporally precise signals to cells. Thus far, the mechanism involved in the photolysis of nanocapsules has been opaque. This paper presents experimental evidence that rules out a photochemical pathway in favor of a photothermal mechanism in the far-red photolysis of dye-sensitized, lipid-vesicle based nanocapsules. Photolysis efficiency was unaffected by the presence of radical inhibitors, and mass spectrometry measurements confirmed that the photolytic process did not produce dye radicals. Measurements of dye quantum yield in the lipid membrane showed an inverse correlation between quantum yield of the dye and photolysis efficiency of the vesicle. The result is consistent with the notion that a decrease in quantum yield translates into more vibrational relaxation and thermal motion of the dye molecules in the membrane and thus more efficient photothermal disruption of the vesicle. Furthermore, we observed that the decrease in quantum yield and increase in photolysis efficiency was caused by the formation of raft-like domains that clustered the dye molecules into concentrated regions. Based on this information, we were able to design new nanocapsules using ternary mixtures of lipid and cholesterol that promoted the formation of raft domains and dye clustering. These nanocapsules showed improved photolysis efficiency over the best results we obtained previously.

INTRODUCTION

Cells exhibit a complex and dynamic organization. To uncover the spatiotemporal dynamics of cellular organization and function, it is often necessary to deliver stimuli to cells with high precision in both space and time. To achieve this, two-photon photolysis of chemically-caged molecules is often used.[1–10] We recently have developed an alternative platform using nanocapsules as physical cages for delivering a wide range of biological molecules to single cells.[11] Physical cages offer several advantages over chemical cages, including fast uncaging times[12–13] and the ability to easily encapsulate a variety of molecules. The subsequent release of molecules from the physical cages to the cell occurs when the physical cage receives an optical trigger, such as a laser pulse.[11–16] We have prepared nanocapsules made from lipid vesicles, hollow silica nanoparticles, and polystyrene-acrylic based hollow beads, all of which can be photolyzed by a single nanosecond UV laser pulse.[12–16]

Recently, we have also demonstrated the ability to photolyze dye-sensitized nanocapsules in the farred region, a feat that thus far is not possible with chemically-caged compounds.[11] This new capability is useful because far-red and near-infrared light is less damaging to biological specimens and has deeper tissue penetration. This strategy of sensitizing nanocapsule shells with chromophores of high absorption cross sections also improves the efficiency of two-photon photolysis.[11]

chiu@chem.washington.edu.

While we showed in all our experiments the ability to photolyze nanocapsules with high efficiency, we had little mechanistic understanding of the photolysis pathway. However, an understanding of the photolysis mechanism is important because it will allow us to design better nanocapsules. Here, we describe our studies on the photolysis mechanism of dye-doped lipid vesicles in the far red (~ 645nm) wavelength region.

We chose dye-doped vesicles for our study because we believe lipid vesicles offer the best overall characteristics for biological applications over those of hollow nanoparticles made from silica or polymers. Lipid vesicles can be easily prepared using a wide range of methods,[11, 16–18] are small (down to a few tens of nanometers in diameter), have thin shells that can be easily dye-doped with photosensitizers,[11–12] have surfaces that are easy to functionalize, and are biocompatible. Nanocapsules based on lipid vesicles, however, do have a short shelf life in comparison to other materials we tested (notably silica and polymer ones), when they are stored in solution (days only versus months for polymer nanocapsules sealed off by thin layers of polyelectrolyte and silica).[14–15] This is an important practical consideration, but we believe we can overcome this issue by an optimized lyophilization procedure.

In our study, we employed the membrane dye, DiD (absorbs maximally at ~ 650 nm), to photosensitize the membrane of our lipid vesicle. We focused on far-red and near-IR photolysis, rather than UV photolysis, because in almost all applications, we believe photolysis in this wavelength region offers better performance and compatibility with the biological system. Upon absorption of light from a single nanosecond laser pulse at 645nm, the DiD-doped lipid membrane is disrupted and releases the encapsulated contents.[11]

The two most likely mechanisms of photolysis are either a photochemical or a photothermal pathway. A photochemical pathway would result in the production of radicals as intermediates, similar to the photolysis of chemically-caged compounds,[4, 5] which then break down the membrane barrier through a radical cascade. A photothermal mechanism would cause a disruption of the membrane from the energy spike derived from the absorption of laser light and subsequent non-radiative decay of the chromophores in the lipid membrane. This paper presents evidence that the mechanism is photothermal. Armed with this information, we are able to design better nanocapsules with a near 100% photolysis efficiency even when using a smaller amount of photosensitizers.

MATERIALS and METHODS

Materials

The mini-extruder used in the generation of vesicles was purchased from Avestin (Ottawa, Ontario). All lipids were purchased from Avanti Polar Lipids, Inc. (Alabaster, AL). Cresyl Violet was purchased from Ana Spec (Fremont, CA). All dyes were purchased from Invitrogen, Molecular Probes (Carlsbad, CA). Capillary pipette tips were purchased from Fisher Scientific (Pittsburgh, PA). All other materials and reagents were purchased from Sigma-Aldrich (St. Louis, MO).

Vesicle formation

Small unilamellar vesicles (SUVs) were formed by extrusion.[11] Chloroform solutions of lipids and membrane dyes were combined in a vial and dried under a stream of N_2 for ~30 min. Samples were then further dried under vacuum for a minimum of two hours to remove any residual chloroform. The dried lipid material was then rehydrated with 50mM borate buffer (pH = 8.5) to a final lipid concentration of 2.0 mM. This solution was then vortexed for about 1 min to remove the lipid cake and to create multi-lamellar vesicles. SUVs were formed by passing the solution of multi-lamellar vesicles through a mini extruder that contained 100nm

pores at a temperature above the melting temperature (T_m) of the lipid membrane for no less than 21 times. Photolysis experiments were carried out immediately after vesicle formation (within 60 min) for consistency. Vesicles used in mass spectrometry (MS) experiments were formed in MilliQ water.

For radical inhibition experiments, all solutions used were bubbled with N_2 for at least 60 min prior to use. Lipid-soluble inhibitors, butylated hydroxyl toluene (BHT) and vitamin E, were added at the initial step prior to removal of the chloroform.

Giant unilamellar vesicles (GUVs) were prepared using electroformation.[17, 18] Chloroform solutions of DiD and lipids were combined and spin-coated onto an indium tin oxide (ITO) coated glass slide. The slides were then placed under vacuum for at least two hours to remove any residual chloroform. The GUVs were formed in MilliQ water using 1 V at 10 Hz for one hour at a temperature above the T_m for the lipids used. Electroformed samples were then diluted 5 fold for viewing.

Single-pulse photolysis of vesicles

Vesicles were subjected to a single pulse (centered at 645 nm) of 3ns duration at varying energies. Vesicle photolysis was determined visually by epi-fluorescence: fluorescence from the visualization membrane dye, 3,3′-dioctadecyloxacarbocyanine perchlorate (DiO-C18), completely disappeared when a vesicle was photolyzed.

Photolysis Efficiency

The photolysis efficiency is defined as the number of successful photolysis events divided by the total number of attempted photolysis events. An attempted photolysis event is the delivery of only a single laser pulse to a single vesicle. A successful photolysis event is an attempted event whereby the vesicle is photolyzed with the single pulse delivered. Three separate days of 100 attempted photolysis events with a fresh batch of vesicles each day were averaged.

Mass spectrometry (MS)

Experiments were carried out on a Bruker Esquire Ion Trap (Fremont, CA). Samples of photolyzed vesicles and controls were injected 10 μL at a time and analyzed in positive ion mode. Samples analyzed in the mass spectrometer were prepared as follows. Coverslips were boiled in a solution containing a 3:2:1 ratio of H_2O:NH_4OH:H_2O_2 for one hour then rinsed and left overnight in a vacuum chamber that contained a small amount (~100μL) of PEG-silane. A 10μL droplet of freshly prepared vesicles were deposited onto the coverslip and subjected to different experimental conditions—photolysis, photobleaching, and a control. For photolysis and photobleaching, we stopped the experiment when ~ 50% of the vesicles were photolyzed or photobleached. The photolyzed vesicles were also subjected to illumination by a blue laser for epi-fluorescence to confirm photolysis; for this reason, vesicles in the control experiment were also subjected to the same amount of blue laser light in epi-fluorescence mode. After each experiment, the 10μL aliquot of vesicle solution was carefully removed from the coverslip using capillary pipette tips. The surface of the coverslip was then washed and collected twice with 10μL isopropanol (IPA), and the entire volume of 30μL was then combined. Complete removal of the vesicles after washing was confirmed by the disappearance of fluorescence from the surface of the coverslip. Samples were then injected into the mass spectrometer for analysis. Triplicates were performed for each set of experiments.

Determination of quantum yields

Quantum yields were determined using a standard cross correlation method. Emission spectra were collected on a Jobin Yvon Fluorolog (Edison, NJ) and absorbance values were collected

with an Agilent UV/VIS spectrometer (Santa Clara, CA). The two standards used were cresyl violet and nile blue.

RESULTS AND DISCUSSION

Optical setup and parameters of vesicle photolysis

Figure 1A shows our optical set up used for both visualizing and photolyzing vesicles. Two continuous wave (CW) lasers, 488nm and 633nm, were used for epi-fluorescence imaging. A N_2 laser was used to pump a solution of the DCM dye (a laser dye) to generate 3ns pulses of 645nm light for vesicle photolysis. A variable neutral density (ND) filter was placed in the beam path of the N_2-pumped dye laser for varying the energy of the laser pulse used to photolyze the vesicles. Additionally, we used an on-stage cell incubator system for controlling the temperature during our photolysis experiments.

For studying vesicle photolysis, we chose a common lipid system of 1,2-dipalmitoyl-*sn*-glycero-3-phosphocholine (DPPC) and 1,2-dipalmitoyl-*sn*-glycero-3-phospho-(1′-*rac*-glycerol) (sodium salt) (DPPG) at a ratio of 9:1. This lipid system is similar to the egg PC (phosphatidyl choline) lipids that were used in our previous publication. Using a defined mixture of synthetic lipids (DPPC:DPPG) rather than a mixture of purified lipids (egg PC) provides for a more consistent vesicle system for our experiments. The photolysis efficiency as a function of dye concentration and laser pulse energy was measured for the DPPC:DPPG lipid vesicles (Figure 1B). This information allowed us to choose the appropriate dye concentration and pulse energy for the type of experiments we conducted and questions we asked. For example, if we wanted to see a decrease in photolysis efficiency, we would choose a dye concentration and pulse energy that gives a ~ 90% efficiency. But if we wanted to determine either an increase or decrease in photolysis efficiency, we would choose a level of dye concentration and pulse energy that corresponded to ~50–60% efficiency.

Evidence against a photochemical mechanism: Radical inhibitors do not affect photolysis efficiency

Our first experiment was modeled after studies that determined the mechanism of chromophore-assisted light inactivation (CALI).[19–21] CALI is a technique that uses radicals generated upon photolysis of chromophores to inactivate proteins that are proximal to the chromophores. Initially, the technique was thought to occur via a photothermal pathway.[21] By conducting radical-inhibition experiments, however, Liao and coworkers determined that the pathway was actually photochemical.[19] Similar to these CALI studies, we photolyzed vesicles in the presence of four radical inhibitors that were also commonly used in the CALI studies. For this study, we used a single 550nJ pulse at 645nm to photolyze 100nm-diameter vesicles of DPPC:DPPG (9:1) with 5.6 mol% DiD; this condition gave us ~ 90% photolysis efficiency (Figure 1B) and thus allowed us to more easily detect any potential decrease in efficiency. For the radical inhibitors, we used two water-soluble ones, sodium azide and mannitol, and two lipid-soluble ones, butylated hydroxyl toluene (BHT) and vitamin E. Prior to each experiment, all solutions were bubbled with N_2 to remove singlet oxygen. One control was performed on vesicles with no radical inhibitors and without bubbling the solutions with N_2. The second control contained no radical inhibitors but was subjected to bubbling with N_2.

Essentially, the presence of radical inhibitors during vesicle photolysis had no statistically detectable effect on the percentage of vesicles photolyzed (photolysis efficiency), even when the radical inhibitors were introduced at high levels (e.g. 200mM NaN_3) (Figure 2). Therefore, while these radical inhibitors had a profound effect on the ability to deactivate protein function by CALI, they did not change the photolysis efficiency of photosensitized lipid vesicles.

Evidence against a photochemical mechanism: Mass spectrometry (MS) measurements

The lack of change in photolysis efficiency in the presence of radical inhibitors provided circumstantial evidence that the mechanism does not involve the formation of radicals. To further confirm this finding, we used MS both to measure any potential decrease in the amount of DiD following photolysis and to detect any photoproducts that may be formed by radicals.

There is an inherent disconnect in the amount of sample required by MS and that generated by single-vesicle photolysis. Our optical technique is designed to photolyze a single vesicle at a time using a focused laser pulse; any defocus of the laser beam will result in too large of a drop in pulse energy to photolyze vesicles efficiently. But MS is a bulk-measurement technique that requires sufficient samples to generate a signal. To address this issue, we developed a specialized procedure where we used a small-volume droplet on top of a microscope coverslip to confine the potential photolysis products.

We used a PEG-silane coated coverslip that ensured molecules could be efficiently washed and removed from the surface for MS analysis (Figure 3A). In our procedure, a 10μL droplet with a concentrated solution of vesicles formed in MilliQ water was placed on a PEG-silane coated coverslip. The vesicles were 100nm in diameter and composed of DPPC, 5.6 mol% DiD, and 1 mol% DiO. Several minutes after the droplet was deposited on the coverslip, most vesicles in solution settled onto the surface and a near monolayer of vesicles coating the surface could be easily visualized. During photolysis, tracks of photolyzed vesicles were easily followed (arrows point to the photolyzed tracks of vesicles in Figure 3B); we photolyzed about 50% of the vesicles. After photolysis, the droplet was picked up with a small-volume pipette tip attachment. The surface of the coverslip was then washed twice with 10μL aliquots of IPA. The IPA aliquots were collected and combined with the vesicle solution. Epi-fluorescence was used to confirm near 100% collection of the vesicles from the surface. Of the now ~30μl solution, 10μl was injected into an ion-trap mass spectrometer for analysis.

At 5.6 mol%, each vesicle contains ~ 1×10^4 molecules of DiD. Photolysis of 50 % of the vesicles would correspond to the generation of ~2.5×10^{16} molecules of potential DiD-derived photoproducts. In 30μl of solution, this would correspond to 0.5 μM of target molecules, which would be sufficient for MS analysis.

To account for any potential variations in day-to-day MS measurements, we used the ratio of DiO to DPPC as an internal standard during each run, and the ratio of DiD to DPPC was investigated under three different conditions (Figure 3C): (1) when vesicles were photolyzed using 645nm pulses, (2) when vesicles were photobleached using the 633nm CW laser, and (3) when no red laser was used (control).

After photolysis of the vesicles, we were unable to detect any photoproducts. Furthermore, the amount of DiD present after photolysis was the same, within error, as that in the control. To ensure that our experiment is sensitive enough to detect a decrease in DiD if radical formation were to occur, we carried out a positive control experiment. Photobleaching of DiD should result in a decrease in the amount of DiD detected by MS. Therefore, we followed the same procedure we used for photolyzing vesicles with the pulsed 645nm laser except we bleached the vesicle using the 633nm CW laser. As anticipated, a significant decrease in the amount of DiD was observed. Taken together, this result (Figure 3C) confirms that DiD did not form radicals upon vesicle photolysis. This finding is consistent with our earlier observation that photolysis efficiency was unchanged in the presence of radical inhibitors. Therefore, we can rule out the photochemical pathway in the photolysis of photosensitized lipid vesicles.

Evidence for a photothermal mechanism

Given the small size of the vesicles and the fact that we needed to photolyze each vesicle individually and sequentially, direct measurements to detect photothermal effects caused by vesicle photolysis were difficult. There are, however, several lines of evidence that support the photothermal pathway. First, we have previously determined that the breakdown time of the vesicle membrane during photolysis is fast:[12, 13] less than 1 μs and may even be less than 300 ns.[13] The typical timescale for the uncaging of chemically-caged molecules via a radical cascade is on the order of many μs to ms.[4] Thus, the fast breakdown time of the vesicle membrane argues against a photochemical mechanism and suggests a photothermal pathway.

Second, if the pathway is photothermal, we would predict an anti-correlation between photolysis efficiency and the quantum yield of the dye: a lower quantum yield translates into a more non-radiative decay of the excited dye molecules that leads to photothermal membrane disruption. We tested this hypothesis using different lipids at different mole percent of DiD. It is evident from Figure 4 that, at a given mole percent of DiD, the higher the quantum yield of DiD, the lower the photolysis efficiency.

There are two factors that contribute to the change in DiD's quantum yield in the different lipid membranes. The first factor simply is a change in lipid alters the micro-environment around the dye and thus the quantum yield. The second factor is caused by the formation of raft domains that concentrates the dye molecules in these domains, which leads to self quenching of the dye and thus a lower quantum yield.

We believe the main factor that affects the quantum yield of DiD and the photolysis efficiency of vesicles is the second one—the formation of domains that result in self quenching of DiD. For example, if we compared the same concentration of DiD in vesicles made with 1,2-di-(9Z-octadecenoyl)-*sn*-glycero-3-phosphocholine (DOPC) to those made with DPPC:DPPG, we saw markedly different photolysis efficiencies (Figure 4A) and quantum yields (Figure 4B). These experiments were carried out at 15 °C. At this temperature, DPPC:DPPG vesicles exist in the solid/gel phase (T_m for both DPPC and DPPG is 41.5 °C) and DOPC vesicles are in the liquid crystalline phase (T_m of DOPC is −20 °C). Liquid crystalline phase permitted a more homogeneous dispersion of DiD throughout the vesicle compared to the solid/gel phase; DiD in the liquid crystalline phase had a higher quantum yield (Figure 4B) and a correspondingly lower photolysis efficiency (Figure 4A).

To confirm this observation, we carried out experiments using a system containing 1,2-dimyristoyl-*sn*-glycero-3-phosphocholine (DMPC) and 1,2-ditetradecanoyl-*sn*-glycero-3-phospho-(1′-*rac*-glycerol) (DMPG) at a ratio of 9:1. This lipid system has a T_m of 23 °C, which conveniently let us to photolyze the vesicles and determine the quantum yield below the T_m (at 15 °C, the temperature set for the room) and above the T_m (at 30 °C, set by a cell incubator system mounted on the microscope stage). The identical lipid system allowed us to rule out any variations caused by the difference in the lipids, such as interaction of the dye with the double bond present in the hydrocarbon tail of DOPC but not DPPC or DPPG. As hypothesized, the photolysis efficiency was significantly higher (and quantum yield lower) when the experiment was carried out below T_m where the vesicles were in the solid/gel phase compared to above T_m where the vesicles exist in the liquid crystalline phase.

To ensure the difference in photolysis efficiency and quantum yield were indeed caused by the formation of raft-like domains, we made GUVs of the DOPC and DPPC lipid systems so we could directly visualize these raft-like domains. GUVs of DPPC with 5.6 mol% DiD contained very small dye domains that are mostly dim due to quenching (Figure 5); these spots became visible when the focus was near the apex of the vesicle (Figure 5A inset). When DOPC GUVs with 5.6 mol% DiD were formed, there was no visible evidence of dye domains (Figure 5B).

Because the quantum yield is inversely proportional to the photolysis efficiency, if the proximity of the dye molecules to each other can be controlled by altering the lipid environment then the photolysis efficiencies should also be tunable.

Promoting formation of raft-like domains and clustering of dye molecules with cholesterol

Armed with the knowledge that the mechanism is photothermal and that the photolysis efficiency depends strongly on the proximity of the dye molecules to each other, we designed a more efficient nanocapsule. When mixtures of lipid systems were formed (Figure 5C and 5D), we began to see spots as the dye localized preferentially into one phase. As the mixture is changed from 1:1 DPPC:DOPC (Figure 5C) to 9:1 DPPC:DOPC (Figure 5D), the spot size became smaller because DiD preferred to locate in the liquid phase provided by DOPC. The preferential partitioning of DiD into DOPC was also supported by our quantum yield measurements of 2 mol% DiD in DPPC vesicles that contained varying amounts of DOPC (Figure 6). As the percent DOPC in the vesicles was lowered, the quantum yield was also lowered because the dye molecules were forced together. The addition of 10% cholesterol had the effect of increasing the solubility of DiD into DOPC domains when low concentrations of DOPC were used.

Vesicles doped with 2 mol % DiD in a lipid membrane of 9:1 DPPC:DOPC + 10% cholesterol had a lower quantum yield than the original DPPC:DPPG vesicles (marked by dotted line). If the photolysis mechanism occurred via a photothermal pathway and the photolysis efficiency was enhanced when the quantum yield of the dye is decreased, then we would expect DiD doped vesicles made of 9:1 DPPC:DOPC + 10% cholesterol to have a higher photolysis efficiency than our original DPPC:DPPG vesicles.

We made 100nm vesicles containing 9:1 DPPC:DOPC + 10% cholesterol and then measured the photolysis efficiencies and quantum yields of these vesicles when they were doped with 2%, 3%, and 4% DiD (Figure 7). As predicted, we achieved a higher photolysis efficiency—98% for 4 mol% DiD in 9:1 DPPC:DOPC + 10% cholesterol versus 91% for 5.6 mol% DiD in 9:1 DMPC:DMPG. A lower DiD concentration using the ternary DPPC:DOPC:cholesterol lipid mixture gave a higher photolysis efficiency than our previous best result with a 9:1 ratio of DPPC:DPPG.

Estimates of heat released

An accurate calculation of the heat generation and release into the lipid membrane of the nanocapsule is not trivial, because it requires knowing how the dye molecules are organized in the membrane. Nevertheless, we provide an order of magnitude estimate below.

The heat generated during capsule photolysis can be estimated by dividing the process into two parts: the amount of energy absorbed by the membrane dyes from the ns laser pulse and the amount of heat dissipated subsequently into the vesicle membrane from the excited dye molecules.

Based on the average percentage of dye molecules in the membrane doped with 5.6% DiD, the duration of the laser pulse (~3ns), the lifetime of DiD (~1–1.5 ns), and taking into account that some DiD molecules will not be optimally oriented for excitation with respect to the laser pulse, we estimate that around 2.4×10^{-15} J of energy will be absorbed by the dye molecules. This is on the order of 50 J/cm^3. This part of the estimate is relatively straightforward.

Determining the heat dissipated into the membrane from the excited dyes is more difficult and can vary significantly depending on how we assume the dye molecules are organized in the membrane. A previous simulation of the location of DiI, a molecule similar to DiD, determined that the dye molecule was buried completely within a DPPC bilayer.[22] Studies have determined

the heat capacity of DPPC to be about 500 J/mol.K at 15°C.[23] Though the heat capacity increases significantly near the T_m value (41.5°C) of the membrane, due to the short pulse duration and fast thermal relaxation times, we assume that the temperature increase is nearly instantaneous so using the heat capacity at 15°C should be sufficient for an estimate. Using these values and assuming the dyes are homogeneously distributed over the membrane, we calculate a ΔT of 33°C averaged over the entire membrane area.

We know, however, that our dye molecules are not homogeneously distributed over the entire membrane. If we average the energy deposited over an area that is half the entire membrane, we reach ΔT of 66°C, and if we assume all the dyes are localized in a single spot, then the maximum temperature increase is around 650°C. From our visualization of the lipid raft domains in large vesicles and from the quantum yield/quenching experiments, we know the dyes are not localized all to the same spot. Thus, ΔT is likely in the neighborhood of 100–200° C.

There are two things to note from this calculation. First, at the length scale (tens of nanometers) and time scale (ns to μs) of our experiments, using equilibrium parameters may not be the most accurate approach to determining the thermal energy involved in capsule photolysis. Patel and Tam determined that for laser pulses in water, heat generation and thermal decay require molecular dynamic simulations, which may be non-trivial to apply to our system.[24] Second, heat dissipation and decay from nanometer-sized objects is very efficient, and thus even if the membrane of the nanocapsule is heated to high temperatures, region that is a short distance away (e.g. ~ μm) should return to ambient temperatures. Indeed, cells survive even if a micron-sized plasma and cavitation bubble is formed on their surface.[25, 26] Nevertheless, we believe an accurate determination of temperature rise in the nanocapsule will require experimental measurements that employ a sufficiently sensitive technique adapted to the length and time scales of capsule photolysis.

Monitoring the quantum yield is an indirect way of observing heat generation during photolysis as quantum yield correlates with the probability of the excited dye molecules relaxing through thermal vibrations rather than emitting a photon. As the quantum yield is decreased, if the mechanism is indeed photothermal, we should see a concomitant increase in the photolysis efficiency due to the increased energy released into the membrane. The quantum yield of membrane dyes can be changed by using lipids that have different solubility for the dye. DiD is more soluble in DOPC than in DPPC membranes, and thus DiD tend to cluster more in DPPC vesicles, which in turn leads to a decrease in quantum yield. As the quantum yield decreased, we saw a corresponding increase in photolysis efficiency as predicted. We can confirm this correlation between quantum yield and photolysis efficiency by using a lipid mixture that contains variable amounts of DOPC and DPPC. Because DiD is more soluble in DOPC, we can control the size of the DOPC domain in the DPPC membrane, and hence the degree of clustering and self-quenching of DiD. Again, we saw the expected increase in photolysis efficiency as the ratio of DPPC to DOPC is changed from 1:1 to 3:1 to 9:1 (Figure 6 and 7).

Photoisomerization

We note another possible pathway for the disruption of the vesicle membrane would be due to photoisomerization of DiD. This phenomenon has been observed in a similar molecule, Cy5, where irradiating the chromophores with 633nm light causes an apparent photobleaching that can be reversed by illuminating the sample with 488nm light.[27] The use of UV photoisomerization of (1,2-bis(4-(4-n-butylphenylazo)phenylbutyroyl)-phosphatidylcholine (Bis-AzoPC) in the membrane of DPPC vesicles has also been demonstrated previously to cause the contained molecules to leak out.[28] This pathway is unlikely to underlie the photolysis of nanocapsules in our experiments, however, for several reasons.

First, release of molecules from vesicles caused by photoisomerization is typically slow. Initiation of release is a few ms at the fastest,[28] which is about 10^3–10^4 times slower than what we reported previously for our system.[12,13] Moreover, the duration of release reported in photoisomerization experiments was also orders of magnitude longer than what we observe for our experiments.

Second, and more importantly, if the photoisomerization mechanism is dominant, then it would be possible to release the contained molecules by adding the effect of multiple laser pulses of low power, where each pulse photoisomerizes a small portion of the dyes in the vesicle membrane. Application of many pulses of low energies results in the progressive conversion of more dyes, which eventually lead to the conversion of a significant population of the membrane dyes to cause leakage from the vesicle; this additive effect has been reported.[28] In contrast, such additive effect is absent in a photothermal mechanism, because thermal excitation will simply dissipate when a laser pulse of insufficient energy is used to photolyze the vesicle. For our experiments, we were never able to achieve photolysis using a train of lower energy pulses, which is consistent with a photothermal pathway but is counter to what would be expected for a photoisomerization mechanism.

Third, the shell of our nanocapsules contains two dyes: DiD that enables nanocapsule photolysis at ~645nm and DiO for visualizing the nanocapsules using 488nm excitation. If photoisomerization is the main mechanism, we would anticipate the nanocapsule to be largely intact while the contained molecules leak through the membrane. In this case, we should still be able to see some DiO fluorescence from the nanocapsules, which we do not for the 100nm diameter nanocapsules we used in our experiments.

Finally, we continuously illuminated the nanocapsule with 488nm light during photolysis in our experiments. In analogy with Cy5, this shorter wavelength illumination should revert DiD back to the original state and we would expect to see recovery and reappearance of the vesicles after photolysis if the mechanism is photoisomerization. In our experiment, the vesicles never re-appeared after photolysis. We also note that we have achieved photolysis of nanocapsules doped with a range of membrane dyes and it is unlikely that these dyes all exhibit efficient photoisomerization to underlie the release of molecules from the capsules. Therefore, we believe the dominant mechanism for photolyzing the nanocapsules is not caused by photoisomerization of the dye molecules, although we cannot rule out that some photoisomerization may be present.

CONCLUSION

Light addressable nanocapsules offer a versatile platform for delivering spatiotemporally defined stimuli to single cells. A wide range of biologically relevant molecules (e.g. metabolites, peptides, proteins, and DNA molecules) can be trapped within nanocapsules based on lipid vesicles, and the optically triggered release of the contents can be spectrally tuned to the far red and near IR to achieve maximal tissue penetration and minimal cellular damage. Until now, the photolysis mechanism of nanocapsules has not been understood. This paper offers evidence that dye-sensitized nanocapsules based on lipid vesicles are photolyzed via a photothermal pathway unlike the photochemical release of chemically-caged compounds. Understanding the photolysis pathway is the first step towards the development of better nanocapsules with higher photolysis efficiencies at a lower concentration of photosensitizer (which may be useful for in vivo experiments) or laser pulse energy (which may be useful for bulk experiments). Furthermore, this difference in photolysis mechanism between chemical cages and nanocapsules has important practical implications: the formation of radicals during the photolysis of chemical cages is toxic to cells. As a result, the use of radical scavengers is often necessary to minimize this harmful side effect of uncaging. The absence of radicals during

the photolysis of nanocapsules is an important and useful feature that is anticipated to broaden their adoption for achieving spatiotemporally precise perturbations of biological systems.

Acknowledgments

The authors would like to thank the Keller Lab for helpful discussions and use of equipment. K.A. acknowledges support from the Center of Nanotechnology at the University of Washington for a UIF and an IGERT fellowship. This work is supported by NIH (AG 029574).

References

1. Pawlicki M, Collins HA, Denning RG, Anderson HL. Angew Chem Intl Ed 2009;48:3244–3266.
2. Gug S, Charon S, Specht A, Alarcon K, Ogden D, Zieta B, Leonard J, Haacke S, Bolze F, Nicoud JF, Goeldner M. Chembiochem 2008;9:1303–1307. [PubMed: 18386275]
3. Neveu P, Aujard I, Benbrahim C, Le Saux T, Allemand JF, Vriz S, Bensimon D, Jullien L. Angew Chem Iintl Ed 2008;47:3744–3746.
4. Adams SR, Tsien RY. Ann Rev 1993;55:755–784.
5. Hishikawa K, Nakagawa H, Furuta T, Fukuhara K, Tsumoto H, Suzuki T, Miyata N. J Am Chem Soc 2009;131:7488–7489. [PubMed: 19438241]
6. Pettit DL, Wang SSH, Gee YR, Augusti GJ. Neuron 1997;19:465–471. [PubMed: 9331338]
7. Li WH. Nat Meth 2006;3:13–15.
8. Furuta T, Wang SSH, Dantzker JL, Dore TM, Bybee WJ, Callaway EM, Denk W, Tsien RY. Proc Natl Acad Sci 1999;96:1193–1200. [PubMed: 9990000]
9. Momotake A, Lindegger N, Niggli E, Barsotti RJ, Ellis-Davies GCR. Nat Meth 2006;3:35–39.
10. Nikolenko V, Poskanzer KE, Yuste R. Nat Meth 2007;4:943–950.
11. Dendramis KA, Allen PB, Chiu DT. Chem Comm 2008;39:4795–4797. [PubMed: 18830496]
12. Sun BY, Chiu DT. J Am Chem Soc 2003;125:3702–3703. [PubMed: 12656592]
13. Sun BY, Lim DSW, Kuo JS, Kuyper CL, Chiu DT. Langmuir 2004;20:9437–9440. [PubMed: 15491172]
14. Sun BY, Chiu DT. Langmuir 2004;20:4614–4620. [PubMed: 15969173]
15. Sun BY, Mutch SA, Lorenz RM, Chiu DT. Langmuir 2005;21:10763–10769. [PubMed: 16262349]
16. Sun BY, Chiu DT. Anal Chem 2005;77:2770–2776. [PubMed: 15859592]
17. Angelova MI, Soleau S, Meleard P, Faucon JF, Bothorel P. Prog Colloid Polym Sci 1992;89:127–131.
18. Veatch SL, Keller SL. Biochim Biophys Acta, Mol Cell Biol Res 2005;1746:172–185.
19. Liao JC, Roider J, Jay DG. Proc Natl Acad Sci 1994;91:2659–2663. [PubMed: 8146171]
20. Horstkotte E, Schroder T, Niewohner J, Thiel E, Jay DG, Hennings SW. Photochem Photobio 2005;81:358–366.
21. Jay DG. Proc Natl Acad Sci 1988;85:5454–5458. [PubMed: 3399501]
22. Gullapalli RR, Demirel MC, Butler PJ. Phys Chem Chem Phys 2008;10:3548–3560. [PubMed: 18548161]
23. Grabitz P, Ivanova VP, Heimburg T. Biophys J 2002;82:299–309. [PubMed: 11751317]
24. Patel CKN, Tam AC. Rev Mod Phys 1981;53:517–550.
25. Shelby JP, Edgar JS, Chiu DT. Photochem Photobiol 2005;81:994–1001. [PubMed: 15850426]
26. Zeigler MB, Chiu DT. Photochem Photobiol 2009;85:1218–1224. [PubMed: 19558419]
27. Heilemann M, Margeat E, Kasper R, Sauer M, Tinnefeld P. J Am Chem Soc 2005;127:3801–3806. [PubMed: 15771514]
28. Morgan CG, Bisby RH, Johnson SA, Mitchell AC. FEBS Lett 1995;375:113–116. [PubMed: 7498457]

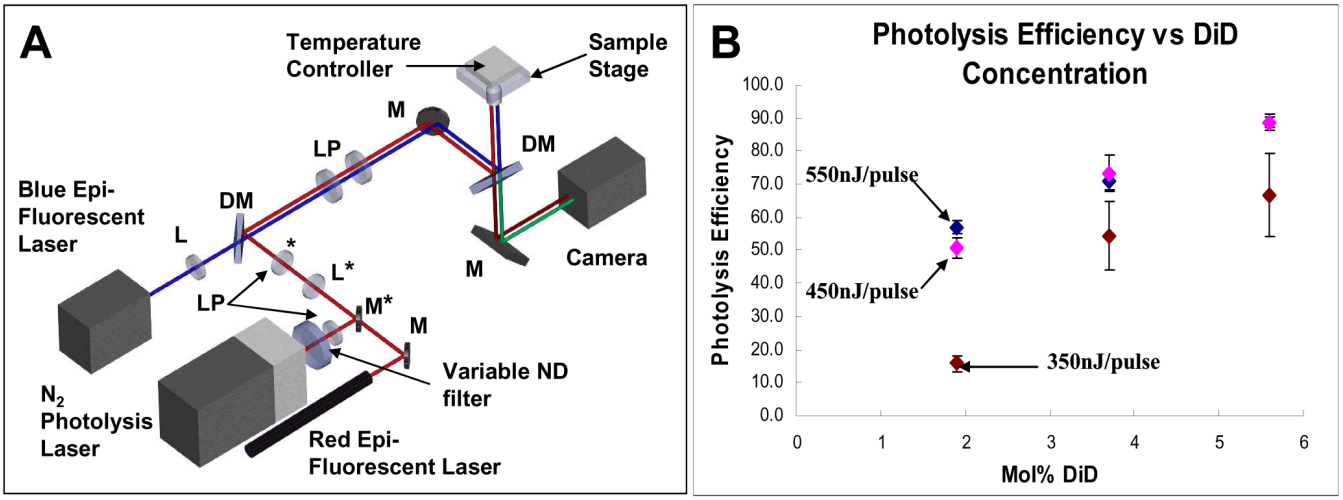

Figure 1.

Optical setup and characterization of nanocapsules. (A) Schematic of optical setup. Items labeled with an asterisk are on flipmounts. [L: lens, LP: lens pair, M: mirror, DM: dichroic mirror, ND filter: neutral density filter] (B) Photolysis efficiencies of vesicles containing varying amounts of DiD using single 3ns laser pulses of 350nJ, 450nJ, and 550nJ energies at ~645nm. Error bars are standard error.

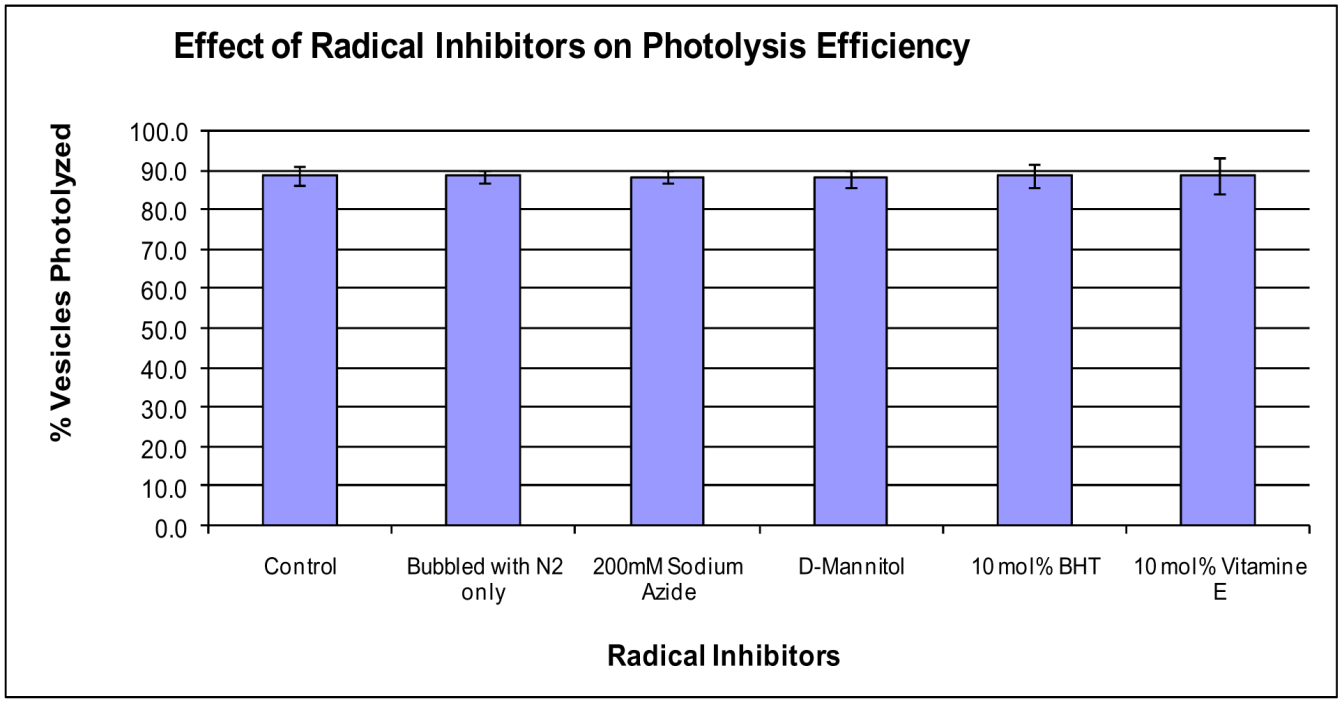

Figure 2.

Photolysis efficiency is unaffected in the presence of radical inhibitors. Photolysis efficiencies of 9:1 DPPC:DPPG + 5.6 mol% DiD vesicles using single 3ns pulses of 550nJ at ~645nm in the presence of different radical inhibitors. Vesicles were formed in a 50mM borate buffer at pH 8.5. Error bars are standard error.

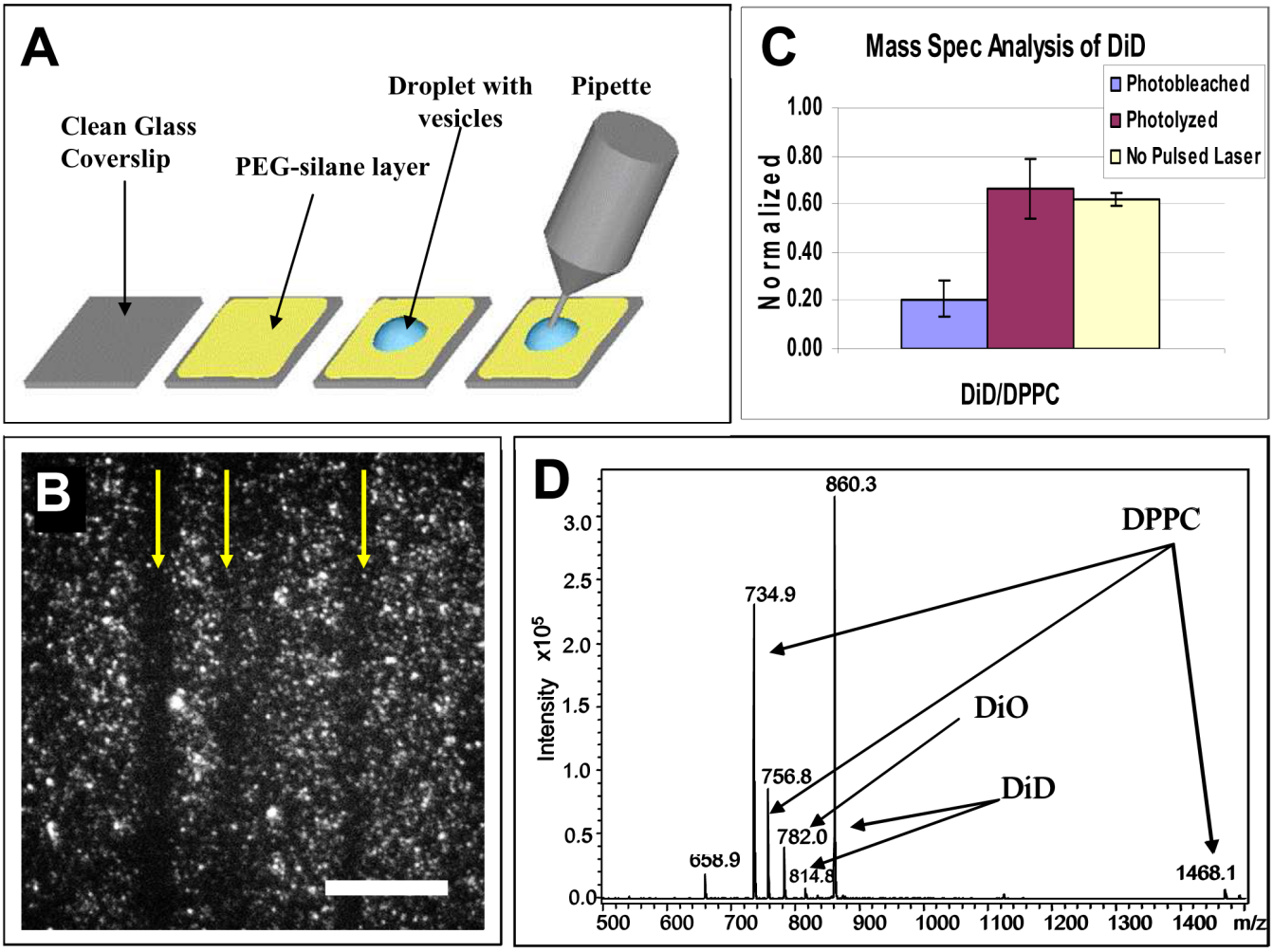

Figure 3.

Mass spectrometry analysis. (A) Schematic of vesicle deposition and collection. A 10μL droplet of vesicles was deposited onto cleaned coverslips coated with PEG-silane. After each experiment, the droplet was collected with a micropipette and combined with solution from two IPA washes of the coverslip surface after vesicle removal. (B) Tracks of photolyzed vesicles on the coverslip surface. Scale bar is 3μm. (C) Ratio of integrated survivor peaks of DiD and DPPC. Error bars are reported as standard error. All vesicles were formed in MilliQ water and contained 5.6 mol% DiD. For the photolysis experiments, vesicles were photolyzed using 550nJ pulses of ~645nm light. For the photobleaching experiment, vesicles were photobleached using a HeNe laser (633nm) at 800μW. In the control experiment, no red laser was used to photolyze or photobleach the vesicles. All powers were measured at the back aperture of the objective. (D) Sample mass spectrum obtained from a control sample of vesicles. The peak at 658.9 was instrument contamination as confirmed by isolation and MS/MS experiments as well as by its presence in blank injections.

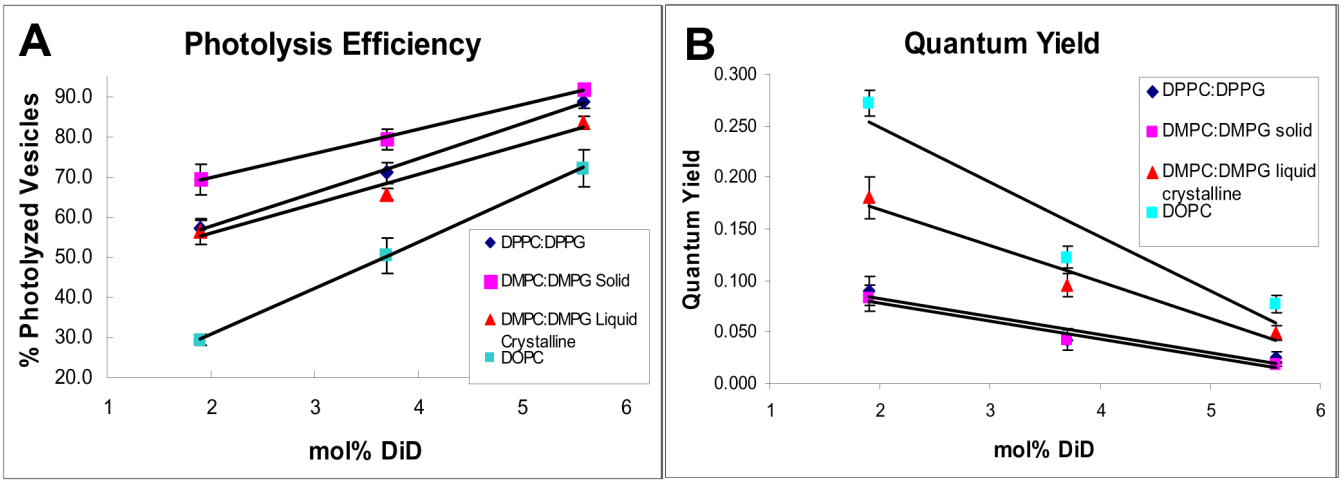

Figure 4.

The photolysis efficiency of vesicles and the quantum yield of dyes in the vesicle membrane are anti-correlated. (A) Photolysis efficiencies of vesicles containing different lipids with 2, 3.7, and 5.6 mol% DiD. Vesicles were photolyzed using single 3ns pulses of 550nJ at ~645nm. For each dye concentration and pulse energy, attempted photolysis was performed on 100 vesicles on 3 separate days for a total N=300 for each data point. (B) Quantum yields of vesicles containing different lipids with 2, 3.7, and 5.6 mol% DiD. DMPC:DMPG vesicles in the liquid crystalline phase are held at a temperature of 30 °C. All error bars are reported as standard error.

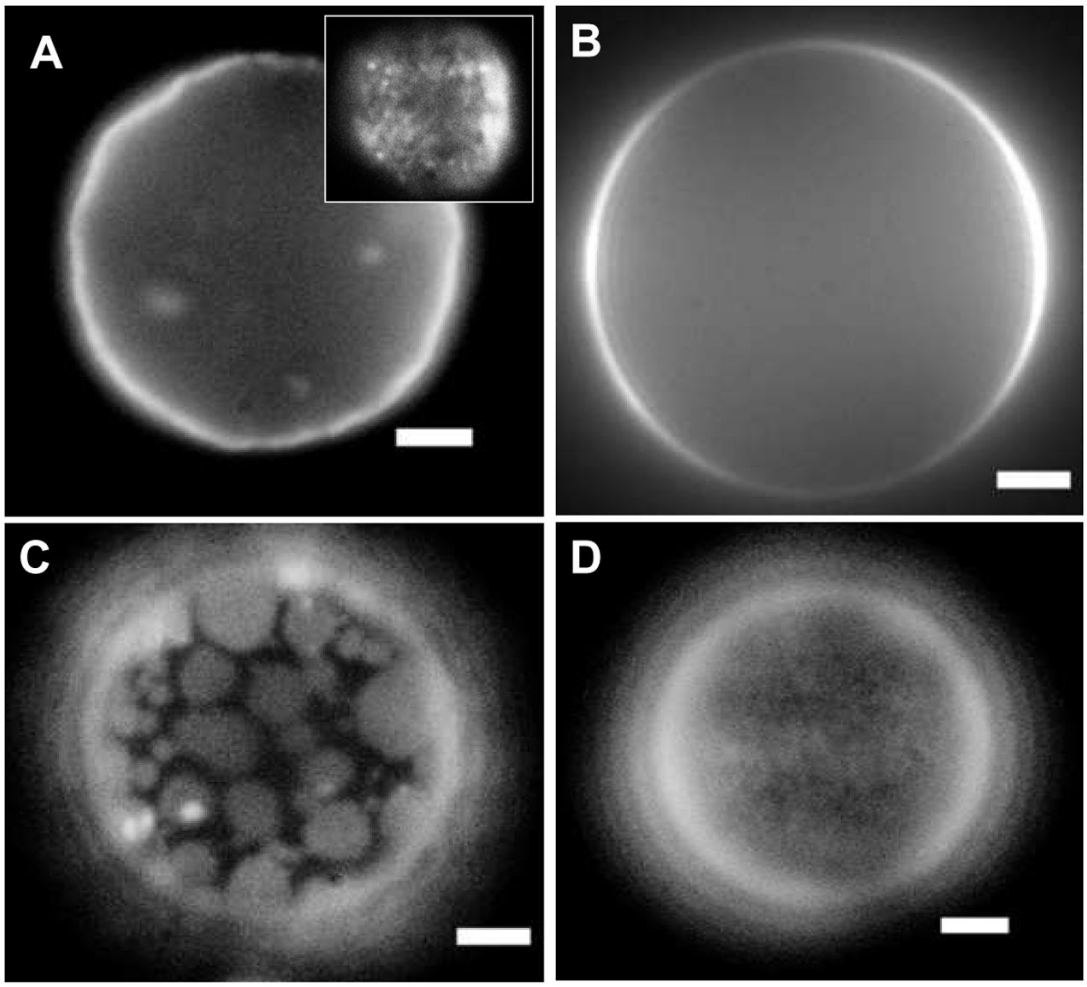

Figure 5.
Fluorescent images of GUVs. GUVs composed of DPPC + 5.6 mol% DiD (A), DOPC + 5.6 mol% DiD (B), 1:1 DPPC:DOPC + 10% Cholesterol + 2 mol% DiD (C), and 9:1 DPPC:DOPC + 10% Cholesterol + 2 mol% DiD (D). The inset in figure A is a view of the same vesicle but focused near the apex. All scale bars are 3μm.

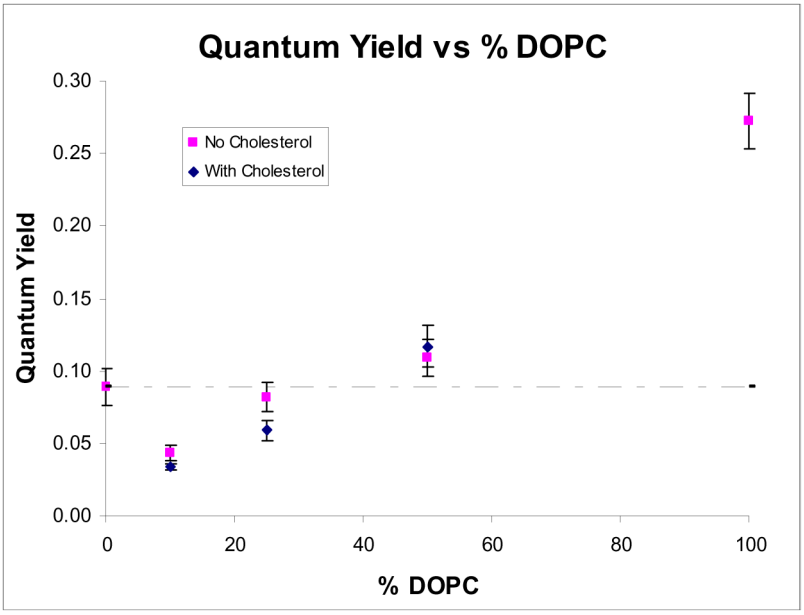

Figure 6.
Quantum yields of DiD in vesicles containing varying percents of DOPC in DPPC. All vesicles were made in a 50mM borate buffer at pH 8.5. The dotted line marks the value of the quantum yield for DPPC:DPPG vesicles.

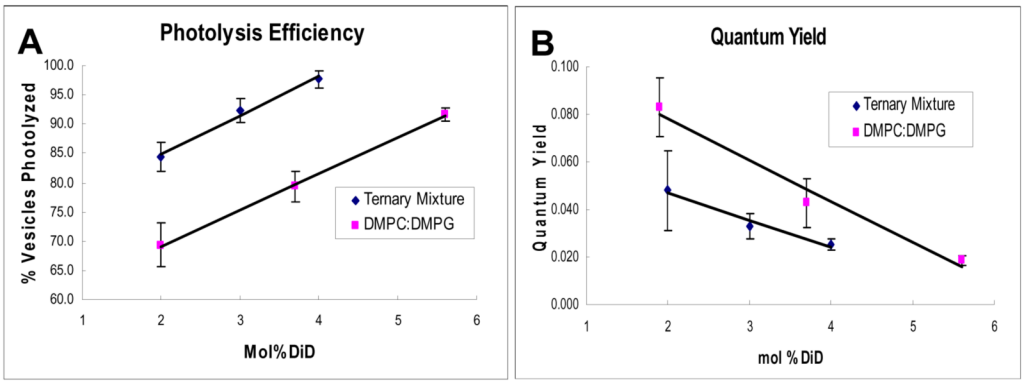

Figure 7.

The use of a ternary lipid mixture to increase the photolysis efficiency of vesicles. (A) Photolysis efficiencies of vesicles of 9:1 DMPC:DMPG and 9:1 DPPC:DOPC + 10% cholesterol with varying amounts of DiD. All vesicles were photolyzed using single 3ns pulses of 550nJ at ~645nm. For each dye concentration, photolysis was performed on 100 vesicles on 3 separate days for a total N=300 for each data point. (B) Quantum yields of vesicles of 9:1 DMPC:DPPG and 9:1 DPPC:DOPC + 10% cholesterol with varying amounts of DiD. All error bars are reported as standard error. All vesicles were prepared in a 50mM borate buffer at pH 8.5.